JOC Article

The Question of Aromaticity in Open-Shell Cations and Anions as Ion-Radical Offsprings of Polycyclic Aromatic and Antiaromatic Hydrocarbons

Sergiy V. Rosokha and Jay K. Kochi*

Department of Chemistry, University of Houston, Houston, Texas 77204

jkochi@uh.edu

Received August 15, 2006

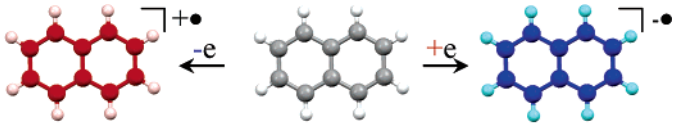

(Cation Radical) (Arene) (Anion Radical)

Arene cation-radicals and anion-radicals result directly from the one-electron oxidation and reduction of many aromatic hydrocarbons, yet virtually nothing is known of their intrinsic (thermodynamic) stability and hence "aromatic character". Since such paramagnetic ion radicals lie intermediate between aromatic (Hückel) hydrocarbons with $4n+2$-electrons and antiaromatic analogues with $4n$-electrons, we can now address the question of π-delocalization in these odd-electron counterparts. Application of the structure-based "harmonic oscillator model of aromaticity" or the HOMA method leads to the surprising conclusion that the aromaticity of these rather reactive, kinetically unstable arene cation and anion radicals (as measured by the HOMA index) is actually higher than that of their (diamagnetic) parent—contrary to conventional expectations.

Introduction

The concept of aromaticity as originally introduced recognizes the unique electronic structures of various polycyclic (Hückel) hydrocarbons in which the π-delocalization of $(4n+2)$ electrons is manifested in unusual stabilities, bond length equalizations, specific magnetic properties, and/or definitive chemical reactivity patterns.[1−5] Moreover, the related idea of antiaromaticity has been invoked to identify $4n$-electron systems with contrasting properties of pronounced bond length alternations, thermodynamic destabilizations, etc.[1,2] Different experimental and theoretical methodologies for the quantitative assignment of aromaticity within the aromatic−antiaromatic paradigm have been developed by thorough analysis of various structural, magnetic, thermodynamics, and kinetics factors.[1,6−9] Moreover, the quantification of extrinsic perturbations such as charge-transfer, hydrogen-bonding, metal complexation, substituent and charge effects, etc.[9−13]

(1) (a) Minkin, V. I.; Glukhovtsev, M. N.; Simkin, B. Ya. *Aromaticity and Antiaromaticity. Electronic and Structural Aspects*; Wiley: New York, 1994. (b) Garratt, P. J. *Aromaticity*; Wiley: New York, 1986.

(2) For the recent thematic issue on aromaticity, see: Schleyer, P. v. R., Ed. *Chem. Rev.* **2001,** *101*, 1115. See also the recent thematic issue on σ- and π-delocalization, see: Schleyer, P. v. R., Ed. *Chem. Rev.* **2005**, *105*, 3433.

(3) Subsequently, the idea of aromaticity was broadened to include heterocyclic compounds,[4a] all-metal clusters,[4b] 3-dimensional molecules,[5] etc.[1,2]

(4) (a) Katritzky, A. R.; Jug, K.; Oniciu D. C. *Chem. Rev.* **2001**, *101*, 1421. (b) Boldyrev, A. I.; Wang, L.-S. *Chem. Rev.* **2005**, *105*, 3716.

(5) (a) Bühl, M.; Hirsch, A. *Chem. Rev.* **2001**, *101*, 1153. (b) Chen, Z.; King, R. B. *Chem. Rev.* **2005**, *105*, 3613.

(6) Cyranski, M. K.; Krygowski, T. M.; Katritzky, A. R.; Schleyer, P. v. R. *J. Org. Chem.* **2002**, *67*, 1333.

(7) (a) Schleyer, P. v. R.; Maerker, C.; Dransfeld, A.; Jiao, H.; Hommes, N. J. R. v. E. *J. Am. Chem. Soc.* **1996**, *118*, 6317. (b) Chen, Z.; Wannere, C. S.; Corminboeuf, C.; Puchta, R.; Schleyer, P. v. R. *Chem. Rev.* **2005**, *105*, 3842.

(8) (a) Schaad, L. J.; Hess, B. A., Jr. *Chem. Rev.* **2001**, *101*, 1465. (b) Cyranski, M. K.; Schleyer, P. v. R.; Krygowski, T. M.; Jiao, H.; Hohlneicher, G. *Tetrahedron* **2003**, *67*, 1657. (c) Cyranski, M. K. *Chem. Rev.* **2005**, *105*, 3773.

(9) (a) Krygowski, T. M.; Cyranski, M. K. *Chem. Rev.* **2001**, *101*, 1385. (b) Krygowski, T. M.; Cyranski, M. K. *PhysChemPhys* **2004**, *6*, 249. (c) Osmialowski, B.; Raczynska, E. D.; Krygowski, T. M. *J. Org. Chem.* **2006**, *71*, 3727. (d) Note that in eq 1, $\alpha/n\sum(R_{opt} - R_i)^2 = f\alpha(R_{opt} - R_{avr})^2 + \alpha/n\sum(R_{avr} - R_i)^2$.

(10) (a) Krygowski, T. M.; Zachara, J. E.; Szatylowicz, H. *J. Org. Chem.* **2004**, *69*, 7038. Krygowski, T. M.; Szatylowicz, H.; Zachara, J. E. *J. Org. Chem.* **2005**, *70*, 8859.

(11) Guell, M.; Poater, J.; Luis, J. M.; Mo, O.; Yanez, M.; Sola, M. *PhysChemPhys* **2004**, *6*, 2552.

(12) Krygowski, T. M.; Stepien, B. T. *Chem. Rev.* **2005**, *105*, 3482.

10.1021/jo061695a CCC: $33.50
Published on Web 11/07/2006

has also provided important insights into the nature of aromaticity.[14]

Let us now address the question of aromaticity in *open-shell* systems with odd numbers of electrons resulting from the removal (and addition) of one electron from both $4n+2$ as well as $4n$ planar π-systems, i.e., cation radicals and anion radicals, respectively, that are known to be the ubiquitous intermediates lying between the classic (diamagnetic) aromatic and antiaromatic hydrocarbons.[15] Indeed, it is becoming increasingly apparent that these arene ion radicals play critical roles in a wide variety of organic redox processes[16] but for which little or nothing is known about their "aromatic character". The latter is quite understandable if one considers that the usual diagnostic probes such as aromatic stabilization energy (ASE), dynamic magnetic (NMR) measurements, etc. are not readily applicable experimentally to such highly charged paramagnetic entities. However, there are several earlier theoretical studies that point to the antiaromatic character of the benzene cation- and anion-radicals,[17,18] together with that of other monocyclic open-shell systems,[19] but the quantitative evaluation of aromaticity in the ion-radicals of other prototypical aromatic hydrocarbons remains unexplored,[20] largely owing to their enhanced reactivities (i.e., kinetic instability),[21] which coupled with their odd-electron distributions severely hinder the experimental measurements of arene ion-radicals.

The recognition of measurable bond length *elongations* and *alternations* accompanying the development of aromatic character dates back to the earliest considerations of aromaticity;[1,22,23] and they provide a direct experimental probe which has been recently developed into the reliable and widely applicable "harmonic oscillator model of aromaticity" or HOMA method,[24] principally by Krygowsky et al.[9] Accordingly, in this study we explore the limits to which such a structure- based methodology can be applied to the aromaticity of arene ion radicals.

The HOMA method is based on the normalized (average) deviation of a given bond length (R_i) from the optimal aromatic value (R_{opt} = 1.388 Å),[25] so that the aromaticity index is calculated via the expression:[9]

$$\mathrm{HOMA} = 1 - \alpha/n\sum(R_{opt} - R_i)^2 = 1 - \mathrm{EN} - \mathrm{GEO} \qquad (1)$$

where n is the number of bonds taken into the summation, and α is the normalization coefficient to make HOMA = 1.00 for an "ideal" aromatic molecule with all bond lengths equal to R_{opt} and HOMA = 0 for hypothetical Kekule structures with the lengths of the CC bonds as in acyclic 1,3-butadiene. Notably, the first term, $\mathrm{EN} = f\alpha(R_{opt} - R_{avr})^2$, represents the decrease of aromaticity related to the increase in bond elongation, where R_{avr} is the average bond length ($f = 1$ if $R_{avr} > R_{opt}$ and $f = -1$ if $R_{avr} < R_{opt}$). The second term, $\mathrm{GEO} = \alpha/n\sum(R_{avr} - R_i)^2$, represents the factor related to bond alternation. As such, the HOMA parameters EN and GEO translate roughly into the classical notions of π-bond elongation and alternation, respectively, which typify the onset of aromatic character.

X-ray crystallographic analysis constitutes the most suitable technique for the precise measurement of bond length effects required for the HOMA method;[26] but the effective crystallization of arene ion-radical salts of sufficient high quality for single-crystal analysis imposes a rather stringent requirement that cannot be met by the ion-radical salts of benzene (or any of its methyl analogues) too reactive to isolate pure. Accordingly, our crystallographic studies in this report necessarily proceed from the more persistent cation- and anion-radicals of naphthalene to anthracene and to their hydrocarbyl derivatives, etc.

In this evaluation of the HOMA index for open-shell systems, we deliberately examine only those structural (bond length) changes accompanying the direct transformation of a given aromatic hydrocarbon into its cation radical and its anion radical to within the requisite accuracy.[26] Thus, such a direct comparison effectively precludes various extrinsic influences on the HOMA index,[27] and allows us to focus solely (or principally) on the effects of one-electron addition and removal relative to a *specific* aromatic parent.

Results

For this structural study, naphthalene ($C_{10}H_8$) represents the simplest aromatic hydrocarbon in which salts of both the cation-

(13) (a) Aihara, J.-I. *Bull. Chem. Soc. Jpn.* **2004**, *77*, 2179. (b) Mills, N. S.; Benish, M. *J. Org. Chem.* **2006**, *71*, 2207.

(14) For example, better bond equalization in aromatic donors with decreased π-electron density in charge-transfer complexes supports the premise that π-electrons are responsible for bond localization and equalization is related to σ-bonds.

(15) (a) Todres, Z. V. *Organic Ion Radicals*: *Chemistry and Applications*; Marcel Dekker, Inc.: New York, 2002. (b) Bauld, N. L. *Radicals, Radical Ions, and Triplets*: *The Spin-Bearing Intermediates of Organic Chemistry*; Wiley: New York, 1997.

(16) (a) Kochi, J. K. *Comprehensive Organic Synthesis*; Trost, B. M., Fleming, I., Ley, S. V., Eds.; Pergamon: New York, 1991; Vol. 7, Chapter 7.4, p 849ff. (b) Rathore, R; Kochi, J. K. *Adv. Phys. Org. Chem.* **2000**, *35*, 193. (c) Rosokha, S. V.; Kochi, J. K. In *Modern Arene Chemistry*; Astruc, D., Ed.; Wiley-VCH: New York, 2002; p 435.

(17) (a) Dietz, F.; Rabinovitz, M.; Tajer, A.; Tyutyulkov, N. *Z. Phys. Chem.* **1995**, *191*, 15. (b) Lindner, R.; Muller-Dethlefs, K; Wedrum, E.; Haber, K.; Grant, E. R. *Science* **1996**, *271*, 1698.

(18) The bond alternation in the X-ray structure of the cation-radical of annulated benzene supports such a conclusion (see section II in the Discussion).

(19) Allen, A. D.; Tidwell, T. T. *Chem. Rev.* **2001**, *101*, 1333.

(20) For evaluation of the aromaticity in some open-shell systems, see: Gogonea, V.; Schleyer, P. v. R.; Schreiner, P. R. *Angew. Chem., Int. Ed.* **1998**, *37*, 1945.

(21) (a) An important differentiation must be made between *thermodynamic* versus *kinetic stabilities*, since reactivity can be related to *persistency* and not necessarily to *instability*, see: Ingold, K. U. In *Free radicals*; Kochi, J. K., Ed.; Wiley: New York, 1973; Vol. 1, p 3ff. Griller, D.; Ingold, K. U. *Acc. Chem. Res.* **1976**, *9*, 13. Such an expressed distinction is generally unnecessary in the theoretical comparisons of aromatic stabilization energy (ASE) of the parent aromatic hydrocarbons. (b) The diagnostic ASE is not easily evaluated experimentally for the highly charged, odd-electron ion radicals since such a thermodynamic assessment lacks the requisite reference point owing to the availability of alternative, easily accessible (kinetics) channels for homolytic, electrophilic, and nucleophilic reactivities. As such, the facile reactions of most paramagnetic cation and anion radicals toward dioxygen, nucleophiles (bases), and electrophiles (acids) can easily mask their inherent (thermodynamics) stability.

(22) (a) Pauling, L.; Sherman, J. *J. Phys. Chem.* **1933**, *1*, 606. (b) Pauling, L. *The Nature of the Chemical Bond*; Cornell University Press: Ithaca, NY, 1960.

(23) Julg, A.; Françoise, P. *Theor. Chim. Acta* **1967**, *7*, 249.

(24) Recent developments of the HOMA method have overcome some drawbacks of earlier structure-based indices[23] and allow reliable quantification of aromaticity, which in the vast majority of cases shows good correlation with other (magnetic- or energy-based) estimates.[6,9]

(25) Using the harmonic potential approach, R_{opt}, corresponds to the minimum-energy point for the compression of the single bond and the expansion of the double bond within 1,3-butadiene.[9]

(26) (a) Nondisordered structures of high precision were included on the basis of the crystallographic *R*-factors of ≤0.07 and the reported mean estimated standard deviation (esd) for the C−C bond length of ≤0.01 Å.[46] (b) Although statistical analysis of naphthalene data did not reveal their correlation with temperature (see Figure S1), the structural data for the HOMA calculations were taken mainly from low-temperature measurements between −100 and −150 °C (see Table S1 for details).

(27) Note: To estimate the effects resulting exclusively from the addition or elimination of an electron (and to exclude substituent effects), the aromaticities of the ion-radicals are compared with those of the parents containing the same substitution patterns.

TABLE 1. Aromaticity (HOMA Index) for Naphthalene and Its Anionic and Cationic Derivatives

	EN	GEO	HOMA
NAP[a]	0.045 ± 0.016	0.129 ± 0.034	0.826 ± 0.025
NAP$^{-\bullet}$[K^+(18-crown-6)$(THF)_2$][b]	0.059 ± 0.009	0.075 ± 0.028	0.866 ± 0.029
NAP$^{-\bullet}$[K^+(cryptand)][b]	0.065 ± 0.005	0.111 ± 0.024	0.824 ± 0.024
NAP$^{-\bullet}$[Na^+(diglyme)$_2$][c]	0.067	0.110	0.823
(**NAP**)$_2^{+\bullet}$(PF_6^-)[d]	0.048	0.041	0.911

[a] Indices and errors calculated as arithmetic mean and standard deviation of corresponding values for 10 structures, see Table S2 in the Supporting Information. [b] This work, deviations calculated from crystallographic esd. [c] Reference 28. [d] Reference 33.

radical and -anion radical are sufficiently persistent[28] to allow direct X-ray crystallographic comparison with the (closed-shell) parent. Notably, the numerous X-ray measurements of naphthalene[29] reveal significant bond alternations within this essentially planar molecule, with the α,β-bond "*b*" being 0.03−0.05 Å shorter than other bonds so that its GEO = 0.136.[9] For comparison, benzene is characterized by completely equalized bond lengths and a HOMA index close to one [the minor deviation from unity being an artifact of the experimental benzene bonds being slightly longer than the value of the "idealized" aromatic bond within the harmonic oscillator model]. Accordingly, the HOMA index of naphthalene (**NAP)** is computed to be lower than that of benzene (**BEN)** as indicated in Chart 1.[9]

CHART 1

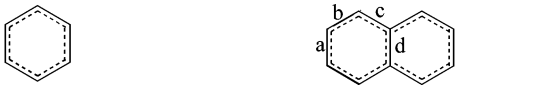

BEN (HOMA = 0.97)[9] **NAP** (HOMA = 0.83)[9]

Furthermore, we also consider various tricyclic hydrocarbons such as anthracene, biphenylene, and phenalenyl for the structure-based comparison of aromaticity of neutral donors relative to their ion-radicals with various odd (11 to 15) numbers of π-electrons. To excise crystal-force effects and to derive statistically reliable conclusions, we compare (i) the same ion-radicals in various crystal lattices with different counterions, (ii) employ noncoordinating counterions to minimize ion-pairing effects, (iii) compare structural data for separated and contact ion pairs,[30] and (iv) evaluate the EN and GEO effects in derivatives containing different substitution patterns.[27]

1. Structural Effects of the Addition/Removal of One Electron to and from Naphthalene and Its Derivatives. 1.A. Unsubstituted Naphthalene. The alkali-metal reduction of naphthalene (**NAP**) under air- and moisture-free conditions in aprotic solvents allows suitable single crystals of its anion-radical to be prepared for X-ray crystallography. In this manner, Bock et al.[28] crystallized **NAP**$^{-\bullet}$ as the complex [Na^+(diglyme)$_2$] salt by reduction with sodium mirror in diglyme solution. Similarly, we reduce naphthalene with potassium-mirror in the presence of the macrocyclic ligands: 18-crown-6 or and [2,2,2]-cryptand (crp) dissolved in tetrahydrofuran to prepare anion-radical salts with [K^+(18-crown-6)$(THF)_2$] and [K^+(crp)] counterions (see the Experimental Section for details). Importantly, the polyether ligands effectively encapsulate the alkali-metal ions to form separated ion-pair salts to largely vitiate electrostatic effects on the anion-radical structure.[30]

The naphthalene moieties in all three anion-radical salts are quite similar, being essentially planar (mean deviation of carbon atoms from the idealized plane of only 0.003 Å) and show markedly shorter "*a*" and "*c*" bonds and longer "*b*" and "*d*" bonds (see Chart 1) as compared to the neutral parent (see Table S1 in the Supporting Information). As a result, the ββ′-bond in **NAP**$^{-\bullet}$ is shorter than the α,β-bond—in contrast to the structure of the neutral parent. Notably, the reverse bond-alternation trends reflect the HOMO and LUMO shapes shown in Chart 2. Indeed, the HOMO is bonding in the α,β-bond "*b*", which is the shortest in the neutral parent. By comparison, the LUMO is bonding relative to the ββ′-bonds, so the population of this orbital in **NAP**$^{-\bullet}$ anion-radical is accompanied by the most significant contraction of the "a" bond.

CHART 2

HOMO **LUMO**

The similar geometries of naphthalene anion-radical within various salts (well-reproduced by ab initio computations)[28,31,32] point to the intrinsic nature (and not crystal forces) as the primary origin of the structure difference from that of the neutral parent, and thus validates the use of the X-ray experimental structures for quantitative comparisons of aromaticity. It is important to note the values of the HOMA index lying in the range in range 0.82−0.87 in Table 1, which is more or less comparable to the HOMA index of naphthalene. Moreover, the similarity of both EN and GEO terms in eq 1 indicates that the addition of one electron to naphthalene does not substantially change either the average bond length or their bond alternation.

While the reduction of naphthalene results in the crystallization of separated anion-radical salts, the corresponding 1-electron oxidation of this aromatic donor leads to the crystallization of the dimeric π-complex in which two naphthalene moieties are crossed at the interplanar separation of 3.2 Å (see Chart 3)[33]

CHART 3

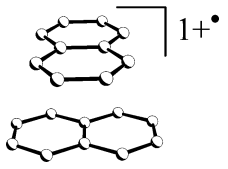

(28) Bock, H.; Arad, C.; Nather, C.; Havlas, Z. *Chem. Commun.* **1995**, 2393.

(29) (a) Ponomarev, V. I.; Filipenko, O. S.; Atovmyan, L. O. *Kristallografiya* **1976**, *21*, 392. (b) Brock, C. P.; Dunitz, J. D. *Acta Crystallogr. B* **1982**, *B38*, 2218. (c) Alt, H. C.; Kalus, J. *Acta Crystallogr. B* **1982**, *B38*, 2595. (d) Oddershede, J.; Larsen, S. *J. Phys. Chem. A* **2004**, *108*, 1057.

(30) Compare: Lu, J. M.; Rosokha, S. V.; Lindeman, S. V.; Neretin, I. S.; Kochi, J. K. *J. Am. Chem. Soc.* **2005**, *127*, 1797.

TABLE 2. Aromaticity (HOMA Index) of Substituted Naphthalene

	R_{avr}, Å	EN	GEO	HOMA
TMN[a,c]	1.405	0.068 ± 0.001	0.133 ± 0.011	0.798 ± 012
	1.405	0.072 ± 0.001	0.128 ± 0.011	0.799 ± 012
TMN$^{-\bullet}$[K^+(cryptand)][a,c]	1.408	0.104 ± 0.002	0.046 ± 0.010	0.850 ± 0.014
	1.407	0.091 ± 0.003	0.051 ± 0.014	0.858 ± 0.014
TMN$^{-\bullet}$[K^+(18-crown-6)(THF)$_2$][a,c]	1.403	0.058 ± 0.005	0.055 ± 0.019	0.887 ± 0.020
	1.404	0.065 ± 0.005	0.063 ± 0.019	0.872 ± 0.019
DMN[b]	1.402	0.053	0.121	0.826
(**DMN**)$_2^{+\bullet}PF_6^-$ [a,c]	1.407	0.097 ± 0.003	0.083 ± 0.021	0.820 ± 0.021
	1.405	0.078 ± 0.003	0.091 ± 0.021	0.831 ± 0.021
OMN[a]	1.413	0.167 ± 0.005	0.192 ± 0.037	0.641 ± 0.038
OMN$^{+\bullet}SbCl_6^-$ [a]	1.419	0.255 ± 0.005	0.056 ± 0.020	0.689 ± 0.020
OON[d]	1.407	0.092	0.104	0.804
OON$^{-\bullet}$[K^+(18-crown-6)(THF)$_2$][a]	1.409	0.109 ± 0.005	0.047 ± 0.016	0.844 ± 0.017
OON$^{+\bullet}SbCl_6^-$ [d]	1.415	0.192	0.005	0.803
OON$^{+\bullet}SbF_6$[e]	1.412	0.138	0.032	0.830
ANA[f]	1.410	0.122	0.157	0.721
ANA$^{+\bullet}SbCl_6^-$ [f]	1.414	0.173	0.063	0.764

[a] This work, deviations calculated from crystallographic esd. [b] Reference 34. [c] Two independent moieties. [d] Reference 35. [e] Reference 33. [f] Reference 36.

CHART 4

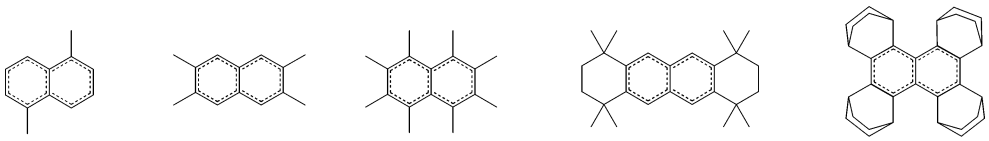

and the overall charge of (+1) for the complex is equally distributed between two equivalent naphthalene entities. The evaluation of their aromaticity via HOMA = 0.911 (Table 1) is somewhat higher than that of either the neutral parent or its anion radical. Further close consideration reveals that the origin of such an increase primarily arises from the better equalization of the bond lengths within the (partially) oxidized constituents resulting in the GEO term being notably lower.

The structural data thus indicate that the addition or (partial) removal of one electron to or from the 10π-electron system has a small effect or may even increase the aromaticity. To check the generality of this conclusion, we also consider analogous effects in various methyl-substituted (and such sterically hindered) naphthalenes as those shown in Chart 4.

1.B. 2,3,6,7-Tetramethylnaphthalene (TMN). **TMN** upon potassium-mirror reduction leads to crystallization of separated ion-pair salts: **TMN**$^{-\bullet}$[K^+(18-crown-6)(THF)$_2$] and **TMN**$^{-\bullet}$[K^+(crp)]. X-ray crystallography of neutral **TMN** and its anion-radicals reveals structural patterns similar to those present in the parent **NAP** (Chart 1). However, the bond alternation in **TMN** with the difference of ~0.05 Å in the $\beta\beta'/\alpha\beta$-bonds is more pronounced than that in the unsubstituted analogue, e.g., the $\beta\beta'$-bond of 1.429 Å in **TMN** is longer than that in **NAP**, Table S1. As a result, the HOMA index of tetramethylnaphthalene in Table 2 is less than that of **NAP** in Table 1. By contrast, in anion-radical salts of **TMN**$^{-\bullet}$, the $\alpha\beta$-bonds are elongated and $\beta\beta'$-bonds are shortened as compared to neutral **TMN** (Table S1), and these result in decreased GEO terms. Taking into account the fact that the average bond lengths of various **TMN**$^{-\bullet}$ moieties remain essentially the same as those in the neutral parent, we find that the attenuation of the GEO term leads to significant increases of the HOMA index in all the anionic species listed in Table 2.

1.C. 1,5-Dimethylnaphthalene. Structural features (Table S1)[34] and the resulting HOMA index of dimethylnaphthalene (**DMN**) listed in Table 2 are similar to those of the naphthalene parent. Thus, the oxidation of this donor with nitrosonium salt results in crystallization of (**DMN**)$_2^{+\bullet}SbCl_6$ (see the Experimental Section) in which the dimethylnaphthalene dimer with (+1) charge is similar to that in Chart 2. Although the two **DMN** moieties are inequivalent, the differences of the corresponding bond lengths are small (Table S1). Thus the aromaticities for both of them are quite similar (Table 2), the HOMA index of the two (partially) oxidized moieties being essentially the same as that in neutral **DMN** (Table 2).

1.D. Octamethylnaphthalene (OMN, Chart 4**).** Earlier crystallographic studies[35 36 37] revealed that the steric repulsions of the methyl substituents in octamethylnaphthalene lead to significant deformation of the naphthalene core. Indeed, its structure (which we remeasured at −100 °C for consistency) shows the marked twisting of the naphthalene framework (Figure 1A) accompanied by a significant deviation of the core (aromatic) carbons from the best plane. This permethylated naphthalene is thus characterized by a higher value of the average bond length and more pronounced bond alternations than those extant in the parent naphthalene (Table S1). As a

(31) For example, Gaussian-98B3LYP/6−311.G* computations[32] result in "*a*", "*b*", "*c*", and "*d*" bond lengths of 1.415, 1.374, 1.418, and 1.431 Å in neutral naphthalene, which compare to 1.388, 1.409, 1.420, and 1.419 Å in the anion radical and to 1.389, 1.404, 1.411, and 1.431 Å in the cation radical.

(32) Pople, J. A. et al. *Gaussian 98W*, Rev. A3.V. 5.0.; Gaussian, Inc.: Pittsburgh, PA.

(33) Le Magueres, P.; Lindeman, S. V.; Kochi, J. K. *Org. Lett.* **2000**, *2*, 3567.

(34) Wilson, C. C. *Chem. Commun.* **1997**, 1281.

(35) Kochi, J. K.; Rathore, R.; Le Magueres, P. *J. Org. Chem.* **2000**, *65*, 6826.

(36) Matsuura, A.; Nishinaga, T.; Komatsu, K. *J. Am. Chem. Soc.* **2000**, *122*, 10007.

(37) (a) Donaldson, D. M.; Robertson, J. M. *J. Chem. Soc.* **1953**, 17. (b) Sim, G. A. *Acta. Crystallogr. B* **1982**, *38*, 623.

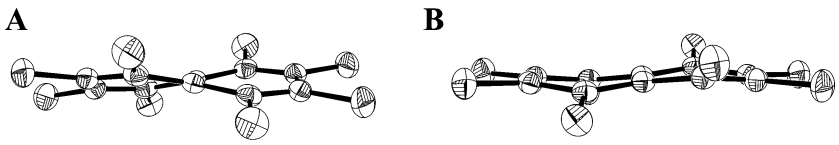

FIGURE 1. Molecular structure of the neutral (A) and the cation-radical (B) of octamethylnaphthalene

result, the values of EN and GEO are both relatively high, and the net HOMA index is rather low (Table 2).

The nitrosonium oxidation of **OMN** donor affords dark crystals of $\mathbf{OMN}^{+\bullet}SbCl_6$ (see the Experimental Section), and X-ray analysis reveals the centrosymmetric "chairlike" geometry of the cation radical (Figures 1B), in contrast to the twisted form of neutral **OMN**. Such a skeletal transformation improves the overall planarity of octamethylnaphthalene—the mean deviation of the carbon atoms in the naphthalene core for the "chairlike" cation radical (0.067 Å) being less than half of the corresponding value for the neutral "twisted" parent (0.160 Å). Importantly, the bond alternation within the $\mathbf{OMN}^{+\bullet}$ cation is drastically reduced relative to that in the neutral donor, and in spite of its longer average bond length and larger EN term (Table 2), the HOMA index for $\mathbf{OMN}^{+\bullet}$ is somewhat higher than that in **OMN** itself.

1.E. Sterically Hindered Naphthalenes. The aromatic core of the sterically encumbered 1,2,3,4,7,8,9,10-octahydro-1,1,4,4,7,7,10,10-octamethylnaphthacene[35] (**OON**, Chart 4) is characterized by a less-pronounced bond alternation and higher aromaticity of HOMA = 0.804 [despite its longer average bond length] as compared to the prototypical tetramethyl-substituted naphthalene. The structure of the $\mathbf{OON}^{-\bullet}$ anion-radical measured as the separated anion-radical salt with $[K^+(18\text{-crown-6})(THF)_2]$ counterion (Experimental Section) shows a slightly increased average bond length in the aromatic core, and further bond equalization leads to a higher overall aromaticity relative to that in the neutral parent (Table 2). Moreover, the oxidation of **OON** results in a structural change similar (but more pronounced) to that observed upon its reduction. Thus, the average bond length in the cation radical measured with two different $\mathbf{OON}^{+\bullet}$ salts[33,35] is about 0.006 Å longer than that in the neutral parent. However, the bond elongation is compensated by their equalization, so that the overall aromaticity index of $\mathbf{OON}^{+\bullet}$ is the same or slightly higher than that of **OON** (Table 2).

The same tendency is observed in the sterically hindered naphthalene fully annulated with a pair of bicyclo[2.2.2]octene rings (**ANA**, Chart 4).[36] Indeed, compared to the neutral donor, $\mathbf{ANA}^{+\bullet}$ is characterized by an elongated average bond length that is more than compensated by bond equalization, so the HOMA index of $\mathbf{ANA}^{+\bullet}$ is even higher than that of **ANA.**

The analysis of the various naphthalene derivatives thus indicates that the aromaticities of the ionic species are the same or higher than that of the corresponding neutral parent with the same substitution pattern. To establish the generality of this observation, and to study further the effects of addition/elimination of an electron, we now turn to extended tricyclic networks.

2. Structural Analysis of Aromaticity in Extended Networks. 2.A. Anthracene and Its Sterically Hindered Derivatives. The structure of anthracene (**ANT**) is characterized by the average bond length of 1.403 Å,[38] which is close to that of naphthalene. However, bond alternation within anthracene is more pronounced—with the shortest "*b*" bonds (Chart 5) being about 1.354 Å and the longest (inner) "*e*" bonds of 1.434 Å (Table S1). Accordingly, the value of HOMA = 0.687 in Table 3is lower than that of unsubstituted naphthalene in Table 1.

CHART 5

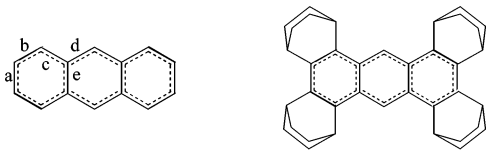

ANT **AAN**

Alkali-metal reduction of anthracene results in the formation of two types of anion-radical salts: first, the separated ion-pairs (SIP), in which the anthracene anion moiety is well-isolated from the countercation by the solvent and/or polyether ligands;[28] and second, the contact ion pair (CIP), in which the alkali-metal cation is directly coordinated to the anthracene moiety.[39] Structural analysis indicates that the addition of one electron to the 14π-electron system leads to a marked elongation of the "*b*" bond (which is the shortest in **ANT**) and shortening of the relatively long "*a*" and "*c*" bonds. Similar to that observed in naphthalene, the geometry changes upon the reduction of anthracene follow the shapes of the HOMO (bonding relative to "*b*" bond) and the LUMO (bonding relative to "*a*" and "*c*" bonds) illustrated in Chart 6.

CHART 6

HOMO **LUMO**

Importantly, the addition of one electron to anthracene results in improved bond equalization in both types (CIP and SIP) of ion pairs, while the average bond length remains essentially unaffected (see Table S1 for details). As a result, the overall structure-based aromaticity calculated from the data from several anion-radical salts is notably higher than that of the neutral hydrocarbon.

The high reactivity of the unsubstituted anthracene cation radical precludes its direct X-ray crystallographic study. We turn to the sterically hindered (annulated) anthracene **AAN (**see Chart 5) for structural information of the neutral and cationic species (Table S1).[36] Thus the oxidation of **AAN** leads generally to bond length changes that are similar to the trends observed in reduction (although the absolute values of the differences are smaller). As such, the better bond equalization overcomes

(38) Brock, C. P.; Dunitz, J. D. *Acta Crystallogr. B* **1990**, *B46*, 795.

(39) Bock, H.; Charagozloo-Hubmann, K.; Sievert, M.; Prisher, T.; Havlas, Z. *Nature* **2000**, *404*, 267.

TABLE 3. Aromaticity (HOMA Index) of Anthracene and Derivatives

	R_{avr}, Å	EN	GEO	HOMA
ANT[a]	1.403	0.058	0.255	0.687
ANT$^{-\bullet}$[K^+(18-crown-6)$(THF)_2$][b]	1.402	0.053 ± 0.009	0.080 ± 0.040	0.867 ± 0.041
	1.401	0.040 ± 0.009	0.067 ± 0.036	0.893 ± 0.037
ANT$^{-\bullet}$[Na^+(diglyme)$_2$][c]	1.407	0.091	0.092	0.818
ANT$^{-\bullet}$[$K^+(THF)_n$][d]	1.401	0.041	0.110	0.848
AAN[e]	1.406	0.085	0.161	0.755
AAN$^{+\bullet}SbCl_6^-$ [e,f]	1.413	0.155	0.037	0.808
AAN$^{+\bullet}SbCl_6^-$ [e,g]	1.413	0.159	0.032	0.808

[a] Reference 38. [b] This work, two independent moieties, deviations calculated from crystallographic esd. [c] Reference 28, SIP. [d] Reference 39, CIP. [e] Reference 36. [f] Planar core. [g] Bent core.

TABLE 4. Aromaticity (HOMA Index) of Phenalenyl Derivatives

	R_{avr}, Å	EN	GEO	HOMA
PHN$^-Li^+$ [a]	1.411	0.138 ± 0.003	0.082 ± 0.025	0.780 ± 0.026
PHN$^-Cs^+$ [b]	1.405	0.078 ± 0.032	0.133 ± 0.040	0.789 ± 0.024
PHN$^\bullet$ [c]	1.403	0.056	0.062	0.882
PHN$^+B(C_6F_5)_4^-$ [c]	1.405	0.070	0.014	0.916

[a] This work, deviations calculated from crystallographic esd. [b] This work, arithmetic mean and standard deviation of corresponding values for 3 independent moieties (Table S3 and ref 41). [c] Reference 0.42.

some increase (and further deviations from the optimal aromatic value) in the average bond length of the cation radical. Consequently, the aromaticity of **AAN**$^{+\bullet}$ is higher than that of the parent (see HOMA index in Table 3). Notably, two independent molecules found in the unit cell of the cation radical are characterized by essentially the same HOMA index, in spite of the fact that one of them is planar, and the other has a deformed anthracenoid core.

2.B. Phenalenyl Radical, Cation, and Anion. The tricyclic phenalene hydrocarbon attracts considerable attention owing to its ability to yield the relatively persistent, highly symmetric (D_{3h}) neutral radical in addition to the diamagnetic anion and cation (Chart 7).[40] Successful preparation and X-ray crystallography of single crystals of 2,5,8-tri-*tert*-butylphenalenyl anion **PHN**$^-$ [41] (see the Experimental Section), together with the radical and cation,[42] provides the opportunity to examine the aromaticity of these 12π-cationic, 13π-neutral, and 14π-anionic species (Table 4).

CHART 7

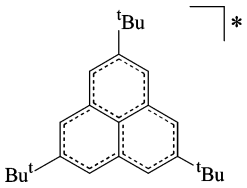

PHN$^-$: * = -

PHN$^+$: * = +

PHN$^\bullet$: * = •

Neutral phenalenyl radical shows a nearly planar geometry with carbon−carbon bond lengths in the ring varying from 1.373 to 1.422 Å (with the external bonds adjacent to *tert*-butyl groups being the shortest, see Table S1).[41] Such bond lengths are comparable to those in naphthalene, and the overall aromaticity (HOMA = 0.882) of this open-shell 13π-electron species is even higher than those observed in naphthalene and anthracene.

CHART 8

The addition and removal of one electron to and from the semioccupied SOMO of phenalenyl (Chart 8) leads to the essentially planar diamagnetic anion (**PHN**$^-$) and cation (**PHN**$^+$), respectively, but does not substantially change the bond length variation pattern (Table S1). In fact, the average bond length of the cation[42] is close to that in the radical. As a result, the decreased bond alternation within the cation leads to a higher aromaticity with HOMA = 0.916 calculated for **PHN**$^+$. In comparison, the **PHN**$^-$ anion shows a somewhat longer average bond length, and more pronounced bond alternation, and as a result, the aromaticity of the 14π-electron anionic species is calculated to be lower than that in either the 12π-electron cation or the open-shell radical.

2.C. Biphenylene and Its Cation- and Anion-Radicals. The 12π-electron biphenylene (**BPH** in Chart 9) contains both (6π-electron) benzenoid and the (4π-electron) cyclobutadienoid skeletons, and these fragments thus reveal prototypical aromatic as well as antiaromatic (structural and magnetic) characteristics.[43]

CHART 9

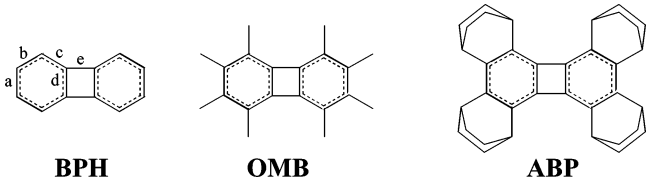

BPH **OMB** **ABP**

The molecular structures of neutral **BPH** and its octamethyl-substituted (**OMB**) and annulated (**ABP**) derivatives (Chart 9) show significant bond alternations, which are especially pronounced in the cyclobutadienoid fragments.[44,45] In fact, the "*e*" bonds (which are 1.512 Å in **BP**, 1.552 Å in **OMB**, and 1.512 Å in **ABP**) are longer than the $C_{ar}-C_{ar}$ bond length (1.490 Å)

(40) (a) Reid, D. H. *Tetrahedron* **1958**, *3*, 339−352. (b) Reid, D. H. *Q. Rev.* **1965**, *19*, 274.

(41) Note that the lower precision in the bond lengths of **PHN**$^-Cs^+$ of ±0.02 Å should be taken into account in its comparison with the other phenalenyl derivatives.

(42) (a) Goto, K.; Kubo, T.; Yamamoto, K.; Nakasuji, K.; Sato, K.; Shiomi, D.; Takui, T.; Kubota, M.; Kobayashi, T.; Yakusi, K.; Ouyang, J. *J. Am. Chem. Soc.* **1999**, *121*, 1619. (b) Small, D.; Zaitsev, V.; Jung, Y.; Rosokha, S. V.; Head-Gordon, M.; Kochi, J. K. J. *Am. Chem. Soc.* **2004**, *126*, 13850.

(43) Mitchell, R. H.; Iyer, V. S. *J. Am. Chem. Soc.* **1996**, *118*, 2903.

(44) Boese, R.; Blazer, D.; Latz, R. *Acta Crystallogr. C* **1999**, *55*, 99000167.

(45) Le Magueres, P.; Lindeman, S. V.; Kochi, J. K. *Organometallics* **2001**, *20*, 115.

TABLE 5. Aromaticity (HOMA Index) of Biphenylene Derivatives

	R_{avr}, Å	EN	GEO	HOMA[g]
BPH[a]	1.420	0.260	0.528	0.212 (0.80/−1.37)
BPH$^{-\bullet}$[Na^+(diglyme)$_2$][b]	1.408	0.099	0.287	0.614 (0.83/−0.26)
OMB[c]	1.422	0.295	0.596	0.109 (0.71/−1.43)
OMB$^{+\bullet}SbCl_6^-$ [d]	1.424	0.327	0.253	0.420 (0.67/−0.51)
OMB$^{+\bullet}SbCl_6^-$ [e]	1.423	0.320	0.276	0.404 (0.66/−0.50)
(**OMB**)$_2^+$ [e]	1.424	0.326	0.401	0.273
	1.423	0.313	0.329	0.358
ABP[f]	1.415	0.188	0.567	0.245 (0.78/−1.11)
ABP$^{+\bullet}SbCl_6^-$ [f]	1.416	0.208	0.272	0.519 (0.73/−0.30)

[a] Reference 44. [b] Reference 47, average over two independent moieties. [c] Reference 45. [d] CH_2Cl_2 solvate, ref 35. [e] Reference 48. [f] Reference 36. [g] In parentheses—HOMA indices for benzenoid and cyclobutadienoid fragments.

measured in various biphenyls.[46] By comparison, the "*d*" bond lengths in the same fragments are about 1.42−1.43 Å in all three analogues (Table S1), and the bond alternations within the benzenoid fragment (of 1.37 to 1.43 Å) are comparable to that observed in naphthalene. In accord with such bond length patterns, the local HOMA index of the benzenoid fragments of neutral biphenylene is about 0.7−0.8, whereas the HOMA index for the cyclobutadienoid ring is negative (see the numbers in parentheses in Table 5). As such, the overall aromaticity of the biphenylene derivatives with HOMA = 0.2 ± 0.1 (Table 5) is significantly lower than the values characteristic of naphthalene, anthracene, and phenalenyl derivatives discussed above.

The structure of the anion-radical of biphenylene[47] (Table S1) is characterized by a significantly shortened (by ∼0.04 Å) "*e*" bond and elongated "*d*" bond, as compared to that in the neutral parent. This results in a marked attenuation of the bond alternation within the butadienoid moiety (and less negative HOMA index). On the other hand, the benzenoid fragments show marked shortenings of the "*b*" bonds (and aforementioned lengthening of the "*d*" bond)—leading to a small increase in their aromaticity. Such changes in the bond lengths again follow the shapes of the frontier orbitals—with the HOMO being bonding with respect to the "*a*" and "*c*" bonds and the LUMO being bonding in the "*b*" and "*e*" bonds as illustrated in Chart 10. This, together with the pronounced changes within the butadienoid fragment, leads to a markedly higher overall aromaticity of the **BPH**$^{-\bullet}$ anion-radical as compared to that of the neutral parent (Table 5).

CHART 10

HOMO **LUMO**

Comparisons of the cation radicals of octamethyl-substituted (**OMB**)[45] and annulated (**ABP**)[36] biphenylenes with the corresponding neutral donors indicate that the one-electron oxidation of biphenylene is accompanied by bond length changes that show similar trends to those observed upon one-electron reduction of **BPH** to **BPH**$^{-\bullet}$. Indeed, the "*b*" bonds and especially the "*e*" bond within the cation radicals are markedly shorter, and the "*a*", "*c*", and "*d*" bonds are longer than those in neutral analogues. Thus, the aromaticity of the cationic species like that of the anion-radical is significantly enhanced relative to that of the corresponding neutral donor—the increase being determined primarily by bond alternation within the butadienoid fragments. It is noteworthy that the cation radicals of octamethylbiphenylene form strong π-complexes with the neutral parent in which the hole (positive charge) is equally distributed between the two constituent moieties. As such, each counterpart bears a (+0.5) charge, and their bond lengths lie approximately midway between that in the neutral donor and that in the cation-radical.[48] Their aromaticity is also enhanced relative to that of neutral **OMB**, but the increase is less than that measured in the cation-radical.

Discussion

Structure-based methodologies such as the "harmonic oscillator model of aromaticity" or HOMA method as applied in this study are potentially very well-suited for the quantitative evaluation to the aromaticity inherent to paramagnetic ion-radicals of aromatic and antiaromatic hydrocarbons because they depend solely on the measurable (carbon−carbon) bond elongations and alternations and are not directly subject to extraneous factors relating to π-electron behavior, stability, etc.—of relevance to other experimental methods.[49] As such, there are two important questions that must be addressed in the application of the HOMA method, as follows.

1. What Are the Uncertainties in the HOMA Measurements? The quantitative application of the structural criterion requires careful evaluation of the accuracy of the calculated values of the HOMA index for aromaticity. This problem is especially relevant for bond length changes derived from X-ray crystallographic data, since the structure variations can result from random as well as systematic errors characteristic of any experimental measurement, as well as from molecular deformations induced by crystal forces. To evaluate the uncertainty in the evaluation of the EN and GEO terms and the HOMA index in eq 1, we first evaluate the errors resulting from the estimated standard deviations (esd) characteristic of X-ray measurements in single structures. We then consider the deviations resulting from instrumental factors and experimental conditions by examining the reports of the same structures from various laboratories and also consider the variations among chemically identical but crystallographically inequivalent species such as different polymorphs, independent molecules within a single unit cell, or for ion radicals, in salts with different counterions. Thus, the uncertainties of X-ray measurements in single structures (esd) lead to the deviations of the HOMA index of about 0.02−0.04 (see Tables 1−4 and the Experimental Section). Overall, the deviations in the EN terms that lie in the range 0.001−0.02 are generally smaller than those of the GEO term of 0.01−0.04.

Numerous reports of the X-ray structure of naphthalene allow us to evaluate the uncertainties resulting from instrumental factors and differences in experimental conditions (Note: only good quality structures with *R*-factors of less than 5% were taken into account). Thus, the data for **NAP** in Table 1 represent the

(46) Allen, F. H.; Kennard, O.; Watson, D. G.; Brammer, L.; Orpen, A. G.; Taylor, R. *J. Chem. Soc., Perkin 2* **1987**, S1−S19.

(47) Bock, H.; Sievert, M.; Bogdan, C. L.; Kolbesen, B. O.; Wittershagen, A. *Organometallics* **1999**, *18*, 2387.

(48) Le Magueres, P.; Lindeman, S. V.; Kochi, J. K. *J. Chem. Soc., Perkin 2* **2001**, *20*, 1180.

(49) Of the commonly available experimental methodologies for the evaluation of aromaticity, the structure-based HOMA index is the uniquely "non-sporting" measure.

arithmetic mean of values calculated for 10 structures taken from the Cambridge Crystallographic Database (see Table S2) and their standard deviations are 0.016 (EN), 0.034 (GEO), and 0.025 (HOMA).

The deviations of the HOMA index calculated for chemically identical but crystallographically inequivalent ionic species are comparable to those for **NAP** (although the number of samples within each set is insufficient for reliable statistical analysis). For example, the arithmetic mean and standard deviation for anion-radicals $\mathbf{NAP}^{-\bullet}$ with three different counterions in Table 1 are HOMA = 0.838 ± 0.024 with EN = 0.063 ± 0.003 and GEO = 0.099 ± 0.020; and $\mathbf{ANT}^{-\bullet}$ in Table 3 are characterized by HOMA = 0.857 ± 0.032, EN = 0.056 ± 0.024, and GEO = 0.087 ± 0.018. Notably, both planar and deformed structures of the sterically hindered anthracene $\mathbf{AAN}^{+\bullet}$ show essentially the same HOMA index (Table 3), and the three independent $\mathbf{PHN}^{-}$ moieties (within the same unit cell) show HOMA = 0.789 ± 0.024 (Table 4).

The foregoing analysis thus indicates that the HOMA index is to be characterized by uncertainties of about ±0.03 for HOMA, ±0.02 for EN, and ±0.03 for GEO. In other words, if the differences of the HOMA index between two species are comparable or less than these limiting uncertainties, we consider them to be related to the accuracy of X-ray measurements and (crystal-force) induced variations, However, we conclude that larger differences are significant, and they are to be associated with the intrinsic structural characteristics of the polycyclic parent and of their ion-radicals.

2. How Does the Odd-Electron Count Affect Aromaticity? While the HOMA indices for naphthalene and its anion-radicals in Table 1 are essentially the same, the corresponding value for the cation-radical in $(\mathbf{NAP_2})^{+\bullet}$ dimer is higher. The latter indicates better bond equalization in the cationic species, such that their GEO = 0.041 is significantly less than that in the neutral parent. [$\mathbf{NAP}^{-\bullet}$ also shows some improvement of bond equalization, but the value is not statistically reliable.] Furthermore, the oxidized or reduced methyl-substituted or sterically hindered naphthalene derivatives in Table 2 are generally characterized by slightly higher R_{avr} and EN terms compared to the neutral parents (although the increases are statistically significant only in $\mathbf{OMN}^{+}$ and $\mathbf{OON}^{+}$ cation-radicals). However, these ion-radicals show better bond equalization and lower GEO terms (e.g., GEO decreases from 0.18 in **TMN** to 0.05 in $\mathbf{TMN}^{-\bullet}$, and from 0.19 in **OMN** to 0.06 in $\mathbf{OMN}^{+\bullet}$). As such, the decreases of the GEO terms of ion-radicals in most cases overcome the increases of their EN values, and the net result is for the HOMA indices of oxidized and reduced ion-radical derivatives to be higher than that of the parent naphthalene.

The anthracene derivatives in Table 3 support the trend observed with the naphthalenes, and the significant improvement of the bond equalization in ion-radicals overcomes some (or slight) increase in the EN term, so the overall HOMA indices of the oxidized or reduced species are higher than that of the neutral parent. We thus conclude for these prototypical polycyclic aromatic hydrocarbons, the addition or removal of one electron to/from the $4n + 2$ electron configurations generally improves their HOMA indices, and this is related to the better bond equalization within their ion-radicals sufficient to neutralize and even overcome some increase of the EN values.[50]

The phenalenyl and biphenylene systems provide further examples of aromaticity in polycyclic conjugated hydrocarbons with different numbers of π-electrons. Thus, the phenalenyl radical and its diamagnetic cation are characterized by higher HOMA indices than that of the anion in Table 4. Notably, both EN and GEO terms in the 13π-electron radical and the 12π-electron cation are better than the corresponding values in the 14π-electron anion. On the other hand, for the biphenylene derivatives in Table 5, the parent neutral hydrocarbon is overall antiaromatic, and their HOMA indices are low (arising from the negative HOMA value in the butadienoid fragments). However, either oxidation or reduction results in a dramatic increase of the HOMA index, and this is related to the improvement of aromaticity in the butadienoid fragments within the ion-radicals, while the index for their benzenoid fragment remains essentially unchanged.

We thus conclude that the HOMA-based aromaticity of the ion-radicals of naphthalene, anthracene, or biphenylene is generally better than that of their diamagnetic parents. Such tendency is not surprising for the ion-radicals of the antiaromatic 12π-electron biphenylene and, indeed, we find the improvements to be largest in these cases. However, in the case of naphthalene and anthracene, the aromaticity of the ion-radicals remains the same or even increases despite the deviations from the classic $(4n+2)$ π-electron configurations. Such a tendency contrasts with earlier conclusions regarding the antiaromatic character of monocyclic 5π- and 7π-electron radicals, which is supported by HOMA = 0.98 for donor and HOMA = 0.61 for the cation radical of the benzene (annulated with the bicyclo[2.2.2]octane frameworks[36]). To explain such a distinction between mono- and polycyclic compounds, we note that the significant deformation of (monocyclic) cation and anion radicals is related to the Jahn−Teller distortion to break the orbital degeneracy.[17] In contrast, the Huckel analysis of naphthalene and anthracene (which takes into account the interactions of some of the carbons with three neighbors) leads to nondegenerate (single) HOMOs and LUMOs. In these cases, the structural changes upon oxidation or reduction appear to follow the shapes of the frontier orbitals.[51] Indeed, the shortest bonds in naphthalene, anthracene, and biphenylene mirror the shapes of their HOMOs in Charts 2, 6, and 10, respectively. Addition or removal of one electron leads to the marked lengthening of these bonds, and shortening of the bonds that reflect the LUMO shapes in Charts 2, 6, and 10. As a result, the bond length alternation in ion-radicals is opposite to that in their neutral parent. Furthermore, the double occupancy of the HOMO in the diamagnetic parent leads to a more pronounced bond alternation, which becomes more diffuse when one electron is either removed from the HOMO or added to the LUMO with a contrasting bonding pattern. This leads to better bond equalization and overcomes the small increase of the average bond length and improves the HOMA index. [Only phenalenyl radical does not change the pattern of bond length alternation upon removal or addition of an electron (which may be related to the nonbonding character of the SOMO in Chart 8[42]).]

(50) Statistical analysis (see Table S4 in Supporting Information for details) indicates that the HOMA indices of anthracene and naphthalene ion-radicals are 0.055 ± 0.024 higher than that of their diamagnetic parents (at 95% confidence level). This improvement is related to the better bond equalization within the ion-radical (the GEO values being 0.088 ± 0.022 lower than that of parents), which overcomes the small rise in average bond lengths in the ion-radicals and increase of the EN values of 0.034 ± 0.017 (see Table S4 in Supporting Information for details).

(51) Calculated (HF/6-311.G*) via Cube = (55, Orbital) option in Gaussian-98.[32]

Conclusion

Analysis of various conjugated aromatic and antiaromatic hydrocarbon leads to the rather unexpected conclusion that the structure-based index for aromaticity of the corresponding polycyclic ion-radicals is generally higher than that of their diamagnetic parent, contrary to the conventional expectations based on their enhanced reactivities.[21] However, we hasten to add that such a conclusion derived from changes in the HOMA index, though quantitative and reliable within the limitations of the X-ray experiments, requires further testing and confirmation by appropriate *theoretical* computations of the more standard measures such as aromatic stabilization energy, dynamic magnetic properties, etc. of arene cation and anion radicals.[52] If so valid, our evaluation of the HOMA index points to the following: (1) the $(4n+2)$ π-electron count is not generally applicable to the odd-electron cations and anions derived from polycyclic (conjugated) hydrocarbons and (2) the reactivity (kinetics) of arene ion-radicals may very well belie their inherent stability (thermodynamics), and vice versa.[21b]

Experimental Section

Octamethylnaphthalene **OMN**,[53] tri-tertbutylphenalene precursor **PHN**-H,[42] and 1,2,3,4,7,8,9,10-octahydro-1,1,4,4,7,7,10,10-octamethylnaphthacene[35] (**OON**) were synthesized as described previously. Tetramethylnaphthalene (**TMN**) was prepared according to modified literature procedure as described in the Supporting Information. The single crystals of neutral **OMN** and **TMN** for X-ray measurements were prepared by slow evaporation of their solution in mixtures of dichloromethane and acetonitrile. Separated ion pair salts of the anion-radical of naphthalene and anthracene derivatives were crystallized via potassium mirror reduction of corresponding neutral molecules **NAP**, **DMN**, **ANT** (from Aldrich) and **TMN** in the presence of polyether ligands 18-crown-6 or cryptand in THF, as described previously.[30] In similar manner, the slow diffusion of hexane into the red solution obtained by the reduction of tri-*tert*-butylphenalene precursor **PHN**-H with an excess of lithium or cesium in THF resulted in crystallization of **PHN**$^-$Li$^+$ and **PHN**$^-$Cs$^+$ salts. [Note: The potassium reduction resulted in crystals with highly disordered structures.] To prepare the crystalline cation-radical salt **OMN**$^{+\bullet}$SbCl$_6$ and the dimeric cation-radical (**DMN**)$_2^{+\bullet}$SbCl$_6$ salts, nitrosonium hexachloroantimonate (NO$^{+\bullet}$SbCl$^-_6$) was added to dichloromethane solutions of the corresponding donor under an argon atmosphere at -30 °C.[54] The diffusion of toluene into these solutions (at -60 °C) resulted in the formation of single crystals suitable for X-ray measurements.

Intensity data were collected with the aid of a Bruker SMART Apex diffractometer equipped with a CCD detector, using Mo Kα radiation ($\lambda = 0.71073$ Å), at -100 °C unless otherwise specified. The structures were solved by direct methods and refined by the full-matrix least-squares procedure.[55] The X-ray structure details are presented in Table S5 in the Supporting Information and can be obtained from Cambridge Crystallographic Data Center.

The EN and GEO terms and the HOMA indices were calculated (with MS Excel program) based on experimental X-ray data according to eq 1. Their standard deviations were calculated (as indicated in footnotes in Tables 1−4) either (i) via the standard expression $\sigma(F) = \sum(\partial F/\partial x_i \times \sigma_i)$, where F represents HOMA, EN, or GEO, x_i are the bond lengths and σ_i are their esd (for X-ray structures in Table S3) or (ii) from statistical analysis of the HOMA indices calculated from structural data for chemically identical, but crystallographically different species. The statistical analysis (including t-test) confirms significant differences between aromaticity indices of ion-radicals and their parents (see Table S4 for details).[50] Note that data in Tables 1−5 result from the rounding of numbers calculated with 5 significant digits (to preserve accuracy).

Acknowledgment. We thank J. Zhang for the synthesis of **TMN** and preparation of single crystals of **TMN** and **TMN**$^{-\bullet}$-[K$^+$(18-crown-6)(THF)$_2$], V. Zaitsev for the synthesis of **PHN** and preparation of single crystals of **PHN**$^-$Li$^+$ and **PHN**$^-$Cs$^+$, D.-L. Sun for the synthesis of **OON** and the preparation of single crystals of (**DMN**)$_2^{+\bullet}$SbCl$_6^-$, J.-M. Lu for the synthesis of **OMN** and the preparation of single crystals of **OMN**$^+$SbCl$_6^-$, T. Y. Rosokha for the preparation of single crystals of **NAP**$^{-\bullet}$[K$^+$(crp)], **NAP**$^{-\bullet}$[K$^+$(18-crown-6)(THF)$_2$], and **OON**$^{-\bullet}$[K$^+$(18-crown-6)-(THF)$_2$], V. Ganesan for preparation of single crystals of **ANT**$^{-\bullet}$-[K$^+$(18-crown-6)(THF)$_2$], S. V. Lindeman for X-ray analysis of **ANT**$^{-\bullet}$[K$^+$(18-crown-6)(THF)$_2$], (**DMN**)$_2^{+\bullet}$SbCl$_6^-$, **PHN**$^-$Li$^+$, and **PHN**$^-$Cs$^+$, I. S. Neretin for X-ray analysis of **NAP**$^{-\bullet}$[K$^+$-(18-crown-6)(THF)$_2$], **NAP**$^{-\bullet}$[K$^+$(crypt)], **OON**$^{-\bullet}$[K$^+$(18-crown-6)(THF)$_2$], and **OMN**$^+$SbCl$_6^-$, S. M. Dibrov for X-ray analysis of **TMN**, **TMN**$^{-\bullet}$[K$^+$(18-crown-6)(THF)$_2$], and **TMN**$^{-\bullet}$[K$^+$(crp)], J.-J. Lu for X-ray analysis of **OMN** and crystallographic assistance, and the R. A. Welch Foundation and the National Science Foundation for financial support.

Supporting Information Available: Synthetic methodology for **TMN** (pp S2−S3), complete ref 32 (p S3), bond lengths for the X-ray structures analyzed in text (Table S1), statistical analysis of the HOMA indices for 10 reported naphthalene structures (Table S2 and Figure S1) and 3 phenalenyl moieties in **PHN**$^-$Cs$^+$ salt (Table S3), statistical analysis of differences in aromaticity indices in ion-radicals relative to their parents (Table S4), and crystallographic parameters and details of the structure refinement (Table S5). This material is available free of charge via the Internet at http://pubs.acs.org.

JO061695A

(52) (a) Indeed, the computation of "aromatic stabilization energy" or ASE[8] with the proper choice of nonaromatic ion-radicals as reference points as well as the Nucleus-Independent Chemical Shift or NICS[7] of the ion-radical would provide an additional theoretical basis for the comparison of their aromaticities relative to those in the diamagnetic parents. (b) Note: The energy-based evaluations of aromaticity (ASE) of ion-radicals relative to their diamagnetic parents involve comparisons of (i) the difference in thermodynamic stabilities of aromatic parent vs their nonaromatic analogues and (ii) the difference in thermodynamic stabilities of the aromatic ion-radical relative to the nonaromatic ion-radical (the same as for the diamagnetic parent, but with one electron added or removed)—in contrast to the direct comparison of the thermodynamic stabilities of the ion-radical and diamagnetic parent.

(53) Hart, H.; Teuerstein, A. *Synthesis* **1979**, *9*, 693.

(54) See: Rosokha, S. V.; Kochi, J. K. *J. Am. Chem. Soc.* **2001**, *123*, 8985.

(55) (a) Sheldrick, G. M. *SADABS* (Ver. 2.03); Bruker/Siemens Area Detector Absorption and Other Corrections, 2000. (b) Sheldrick, G. M. *SHELXS 97*, Program for Crystal Structure Solutions; University of Göttingen: Göttingen, Germany, 1997.(c) Sheldrick, G. M. *SHELXL 97*, Program for Crystal Structure Refinement, University of Göttingen: Göttingen, Germany, 1997.